ELSEVIER

Journal of Fluids and Structures 20 (2005) 189–195

JOURNAL OF FLUIDS AND STRUCTURES

www.elsevier.com/locate/jfs

Aeroelastic analysis of panels in compressible flows

A.L. De Bortoli*

UFRGS-PPGMAp-Bento Gonçalves 9500, P.O. Box 5080, UFRGS-PPGEQ-Rua Luiz Englert s/n, 90040-040, Porto Alegre-RS, Brazil

Received 26 April 2002; accepted 24 October 2004

Abstract

This work develops a method to solve fluid–structure problems based on the arbitrary Lagrangian–Eulerian, ALE, formulation using the central finite difference, explicit Runge–Kutta time-stepping scheme. This model builds on earlier ones that involve ALE with finite elements instead of finite differences, in order to obtain higher-order space and time approximations which are necessary for some aeronautical applications. Numerical tests are carried out for an airfoil and a panel using the Euler equations with Mach numbers ranging from 0.2 to 2.0 and the results are shown to compare favourably with available data found in the literature.

1. Introduction

Due to weight restrictions in modern aircraft their structure needs to be more flexible and, consequently, aeroelasticity plays an important role. Aeroelasticity is the study of the mutual interaction that takes place between the inertial, elastic and aerodynamical forces. There are many important aeroelastic phenomena, such as flutter and divergence (Bisplinghoff et al., 1957; Försching, 1974).

The aeroelasticity methods can be classified as weakly and strongly coupled methods (Guruswamy, 1990; Marshall, 1996). A more complete mathematical modelling of the problem results in a strongly coupled scheme.

This work develops a numerical method for the solution of aeroelastic problems based on the ALE formulation. The central finite difference explicit Runge–Kutta time-stepping scheme is employed to solve for Mach numbers ranging from 0.2 to 2.0 about a panel. It is convenient to use the momentum equations to obtain the velocity components, the energy equation for the total energy, the mass conservation for the density and the state relation for the pressure.

Here a panel is considered to be a surface of moderate curvature submitted to flow over one of its faces and free on the other. It is an important dynamical model because experiments suggest that when it is clamped at one end and free at the other it behaves essentially as a dynamical airfoil. It can be stable or unstable, depending on the incident flow velocity. If it is simply supported or clamped at both ends; it can lose stability by divergence at subsonic flows or flutter at supersonic flows (Garrad and Carpenter, 1982). However, a panel with a clamped end and free elsewhere loses stability by flutter at subsonic flows and by divergence at supersonic flows.

Results obtained for Euler equations are compared to potential equation solutions based on the conformal mapping method (Blazek, 1994) and with an aeroelastic model.

*Tel.: +55 51 3316 6189; fax: +55 51 3316 7301.
E-mail address: dbortoli@mat.ufrgs.br (A.L. De Bortoli).

0889-9746/$ - see front matter © 2004 Elsevier Ltd. All rights reserved.
doi:10.1016/j.jfluidstructs.2004.10.011

2. Governing equations

The solution is advanced in time obtaining the structural displacements with the fluid pressures at same time-step. The Euler equations are written for unsteady compressible bidimensional inviscid flows in differential form (Kroll and Rossow, 1989) based on ALE (Belytschko and Hughes, 1986; Souli et al., 2000) formulation as

mass equation:

$$\frac{\partial(\rho J)}{\partial t} = J\frac{\partial}{\partial x_j}[\rho(w_j - v_j)]; \tag{1}$$

momentum equation:

$$\frac{\partial(\rho v_i J)}{\partial t} = J\frac{\partial}{\partial x_j}[\rho v_i(w_j - v_j)] + J\left(\rho b_i - \frac{\partial p}{\partial x_i}\right); \tag{2}$$

energy equation:

$$\frac{\partial(\rho E J)}{\partial t} = J\frac{\partial}{\partial x_j}[\rho E(w_j - v_j)] + J\left(\rho v_j b_j - \frac{\partial(p v_j)}{\partial x_j}\right); \tag{3}$$

where w_j is the reference frame velocity, v_j the fluid velocity, ρ the fluid density, p the pressure, E the total energy, b_i the body force and $J(x_0, t) = \partial V/\partial V_0$ provides the mathematical link between the current volume $\mathrm{d}V$, function of the mixed variables, and the associated volume $\mathrm{d}V_0$, function of the material coordinates.

In order to close this system of equations the state relation for a perfect gas is employed

$$p = \rho RT = (\gamma - 1)\rho\left[E - \frac{u^2 + v^2}{2}\right], \tag{4}$$

where R is the gas constant, γ the specific heat ratio and T the temperature. Note that, taking the reference velocity w_j equal to zero, the Eulerian formulation is obtained; while taking $w_j = v_j$, the purely Lagrangian formulation is reached. This set of equations can be written as follows:

$$\frac{\partial \mathbf{W}}{\partial t} = J\frac{\partial \bar{\mathbf{F}}}{\partial x_j} + \mathbf{S}, \tag{5}$$

where $\mathbf{W}$ is the vector of convective variables, $\bar{\mathbf{F}}$ the convective flux tensor and $\mathbf{S}$ the pressure and other source terms.

3. Solution procedure

In the computational domain the cell vertices are identified by their indices (i,j). As Eq. (5) is valid for an arbitrary cell, it can be written as (Kroll and Rossow, 1989)

$$\frac{\partial \mathbf{W}_{i,j}}{\partial t} = -\mathbf{Q}_{i,j}. \tag{6}$$

When one solves the Euler equations using a central averaging nondissipative scheme, it is advised to introduce some artificial dissipation (Kroll and Rossow, 1989). The optimum amount of artificial viscosity is mainly determined not by stability considerations, but by the smoothing properties of relaxation. The reduction of nonsmooth error components is basically a local task whose process efficiency can be measured by local mode analysis. The dissipation vector $\mathbf{D}_{i,j}$ is introduced as follows:

$$\frac{\partial \mathbf{W}_{i,j}}{\partial t} = -[\mathbf{Q}_{i,j} - \mathbf{D}_{i,j}]. \tag{7}$$

The dissipation operator is a blend of second- and fourth-order differences and is defined, according to Jameson et al. (1981) as

$$\mathbf{D}_{i,j} = \mathbf{d}_{i+\frac{1}{2},j} - \mathbf{d}_{i-\frac{1}{2},j} + \mathbf{d}_{i,j+\frac{1}{2}} - \mathbf{d}_{i,j-\frac{1}{2}}, \tag{8}$$

where the dissipation coefficient is given by

$$\mathbf{d}_{i+\frac{1}{2},j} = \alpha_{i+\frac{1}{2},j}[\varepsilon^{(2)}_{i+\frac{1}{2},j}\delta_x \mathbf{W}_{i,j} - \varepsilon^{(4)}_{i+\frac{1}{2},j}\delta_{xxx}\mathbf{W}_{i-1,j}]. \tag{9}$$

The dissipation flux $\mathbf{d}_{i+\frac{1}{2},j}$ is of third order in smooth regions; while in regions of high-pressure variations, the dissipation is of first-order and the scheme behaves as a first-order upwind scheme. The difference operators of first and third order are δ_x and δ_{xxx}, respectively: $\delta_x \mathbf{W}_{i,j} = \mathbf{W}_{i+1,j} - \mathbf{W}_{i,j}$, $\delta_{xxx}\mathbf{W}_{i,j} = \mathbf{W}_{i+2,j} - 3\mathbf{W}_{i+1,j} + 3\mathbf{W}_{i,j} - \mathbf{W}_{i-1,j}$.

The scaling factor α is written for the **i** direction according to Blazek (1994) as

$$\alpha_{i+\frac{1}{2},j} = \frac{\lambda^{i^*}_{i,j} + \lambda^{i^*}_{i+1,j}}{2}, \tag{10}$$

where the eigenvalues, λ, are scaled in each coordinate direction as

$$\lambda^{i^*}_{i,j} = \lambda^{i}_{i,j}\phi^{i}_{i,j}, \tag{11}$$

considering the cell aspect ratio

$$\phi^{i}_{i,j} = 1 + \left(\frac{\lambda^{j}_{i,j}}{\lambda^{i}_{i,j}}\right)^{\psi}, \tag{12}$$

where $\psi = \frac{2}{3}$ is a parameter used to scale the spectral radii.

The coefficients adapted to the local pressure gradients $\varepsilon^{(2)}$ and $\varepsilon^{(4)}$, which we needed to obtain the dissipation coefficient, are written as follows:

$$\varepsilon^{(2)}_{i+\frac{1}{2},j} = k^{(2)} v_{\max}, \tag{13}$$

$$\varepsilon^{(4)}_{i+\frac{1}{2},j} = \max(0, k^{(4)} - \varepsilon^{(2)}_{i+\frac{1}{2},j}), \tag{14}$$

where the divided second-order pressure sensor is given by

$$v_{i,j} = \left|\frac{p_{i+1,j} - 2p_{i,j} + p_{i-1,j}}{p_{i+1,j} + 2p_{i,j} + p_{i-1,j}}\right| \tag{15}$$

with $v_{\max} = (v_{i+2,j}, v_{i+1,j}, v_{i,j}, v_{i-1,j})$ and $k^{(2)}$ and $k^{(4)}$ are $0.5 \leqslant k^{(2)} \leqslant 0.6$, $\frac{1}{128} \leqslant k^{(4)} \leqslant \frac{1}{48}$.

In order to integrate equations in time the Runge–Kutta method is chosen, characterized by its low operation count; more than two stages are employed to extend its stability region. The multistage scheme, requiring few computational storage, is written as

$$\mathbf{W}^{(0)}_{i,j} = \mathbf{W}^{n}_{i,j}, \tag{16}$$

$$\mathbf{W}^{r}_{i,j} = \mathbf{W}^{(0)}_{i,j} - \alpha_r \Delta \mathbf{t} \mathbf{R}^{(r-1)}_{i,j}, \tag{17}$$

$$\mathbf{W}^{n+1}_{i,j} = \mathbf{W}^{(r)}_{i,j}, \tag{18}$$

where $\mathbf{W} = (\rho J, \rho u J, \rho v J, \rho E J)^{\mathrm{T}}$ and

$$\mathbf{R}^{r}_{i,j} = \mathbf{Q}^{r}_{i,j} - \mathbf{D}^{(r)}_{i,j} \tag{19}$$

with $r = 0, 1, 2, \ldots, m = 5$ and the following second-order coefficients: $\alpha_1 = \frac{1}{4}$, $\alpha_2 = \frac{1}{6}$, $\alpha_3 = \frac{3}{8}$, $\alpha_4 = \frac{1}{2}$, $\alpha_5 = 1$.

4. The fluid–structure coupling and code calibration

Since the aeroelastic deformation resulting from the flexibility of an aerodynamic body can change the flow conditions considerably, it is convenient to use the ALE approach. The conditions prescribed at each point of the interface between an inviscid fluid and a deforming structure are (Belytschko and Hughes, 1986):

(i) the coincidence of grid velocity w_j of the fluid with the solid velocity;

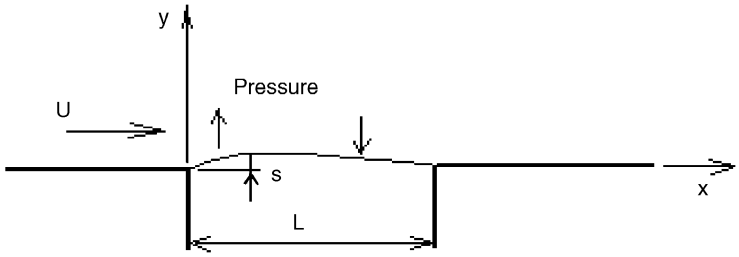

Fig. 1. Aeroelastic panel model.

(ii) the coincidence of normal velocity of the fluid with that of the solid;
(iii) the tangential velocity of the fluid is unconstrained.

To compare to the solutions to be obtained, a panel model is given in Fig. 1. The simplified equation for this problem is

$$\frac{\partial^4 s}{\partial x^4} + \frac{\rho_s h}{D}\frac{\partial^2 s}{\partial t^2} + \frac{\Delta p}{D} = 0, \tag{20}$$

where

$$\Delta p = -\rho\left[\frac{\partial \phi}{\partial t} + U\frac{\partial \phi}{\partial x}\right]_{y=0}. \tag{21}$$

In Eqs. (20) and (21) Δp is the local fluid pressure difference, U the mean fluid velocity, $D = Eh^3/[12(1-\nu^2)]$ the flexural rigidity, h the panel thickness, ρ the fluid density, ρ_s the material density, and ϕ the potential velocity perturbation satisfying the equation

$$\frac{\partial^2 \phi}{\partial x^2} + \frac{\partial^2 \phi}{\partial y^2} = 0, \tag{22}$$

with the boundary conditions

$$\left[\frac{\partial \phi}{\partial x}\right]_{y=0} = \frac{\partial s}{\partial t} + U\frac{\partial s}{\partial x} \text{ for } 0 < x < L,$$

$$\left[\frac{\partial \phi}{\partial x}\right]_{y=0} = 0 \text{ elsewhere.}$$

The analytical solution results in the following critical parameter (Garrad and Carpenter, 1982)

$$\lambda^2 = \frac{\rho U^2 L^3}{D}, \tag{23}$$

with $\lambda = 181$ for a clamped panel and $\lambda = 41.8$ for a simply supported panel (Garrad and Carpenter, 1982). In this way, a clamped steel panel of 1 m length has a critical thickness of about 1.54 mm at Mach number 0.3; almost incompressible flow.

5. Numerical results

One way of proving the validity of the numerical Euler solutions is to compare them with potential solutions or experimental data. This is done before analysing the coupling of fluid and structure.

Numerical results for NACA 0012 were obtained using a C-grid topology of 256×64 cells. The position of the outer boundary is chosen around 20 chord lengths away from the airfoil and the far field boundary condition is modified due to a vortex (Usab and Murman, 1983; Blazek, 1994).

The conditions imposed at the outer boundary should assure that the outgoing waves are not reflected back into the flow field. Inappropriate conditions can substantially degrade the accuracy of the computed solution and slow down the

convergence. The far-field potential is strictly valid in subsonic flows; however, the correction of the free-stream conditions is applied in transonic flows and has been proved helpful in this regime also.

Fig. 2 shows the pressure contours and coefficient computed for Mach = 0.3 and $\alpha = 5^\circ$; Fig. 3 the pressure contours for Mach = 0.754 and $\alpha = 2^\circ$ and Mach = 0.8 and $\alpha = 1.25^\circ$ (De Bortoli, 1994). Numerical solutions for Euler equations are in good agreement with experimental (Kroll and Rossow, 1989) or numerical/theoretical data (Blazek, 1994). The pressure coefficient differs by less than 5% compared to the conformal mapping solution (Blazek, 1994), which is expected for Mach = 0.2; such difference decreases for small Mach numbers (De Bortoli, 1994). The code showed itself to be efficient also to obtain shocks over aerodynamical surfaces.

In the following, numerical solutions for a panel subjected to subsonic, transonic and supersonic flows, Mach = 0.3, 0.8 and 2.0, are presented. A panel is chosen because experiments suggest that when it is clamped or simply supported at its ends it behaves essentially as a dynamical airfoil (Garrad and Carpenter, 1982). The grid contains 60×24 cells; 20 divisions over the curved surface.

Fig. 4 shows the pressure coefficient lines for Mach = 0.3, 0.8 and 2.0, for a panel based on the NACA 0012 airfoil, whose y coordinate was divided by 3, resulting in a 2% surface curvature. The panel has unit length, going from 2 to 3 in the coordinate system. The pressure coefficient lines are in agreement with the expected solution; besides which changing the panel surface to the geometry of an airfoil or a cylinder gives the corresponding standard solutions.

The aeroelastic solutions obtained using the Euler equations are plotted in Fig. 5; the numbers 1–8 indicate the panel position after the corresponding number of time units of 0.1 s. The panel thickness corresponds to 2 times its critical value; therefore displacements are small.

Observe that the panel vibrates reaching the first structural mode for subsonic flow and the second mode for supersonic flow. This suggests that the system tends to lose stability by divergence at subsonic flows and by flutter at supersonic flows, when its thickness is less than the critical value.

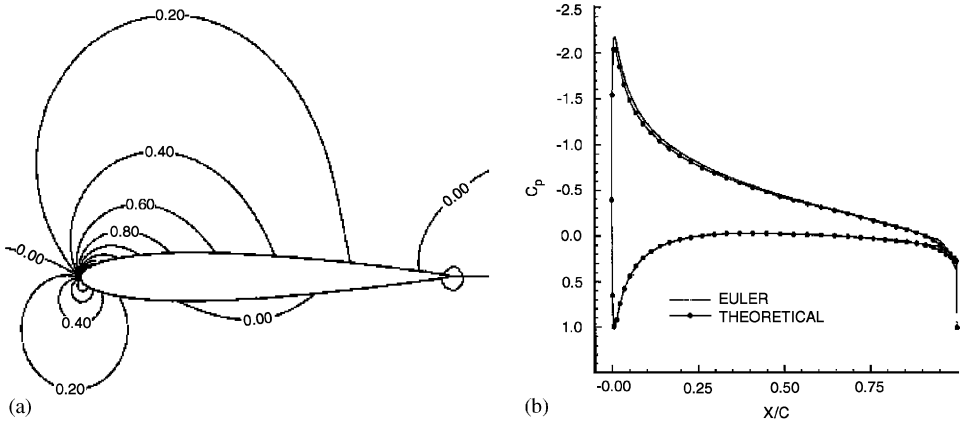

Fig. 2. Pressure contours (a) and coefficient (b) for NACA 0012, Mach = 0.2 and $\alpha = 5^\circ$.

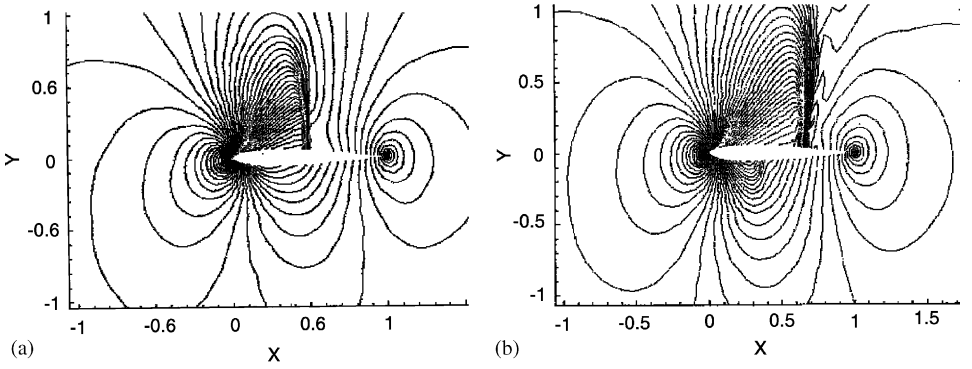

Fig. 3. Pressure contours for NACA 0012: (a) Mach = 0.754 and $\alpha = 2^\circ$, (b) Mach = 0.8 and $\alpha = 1.25^\circ$.

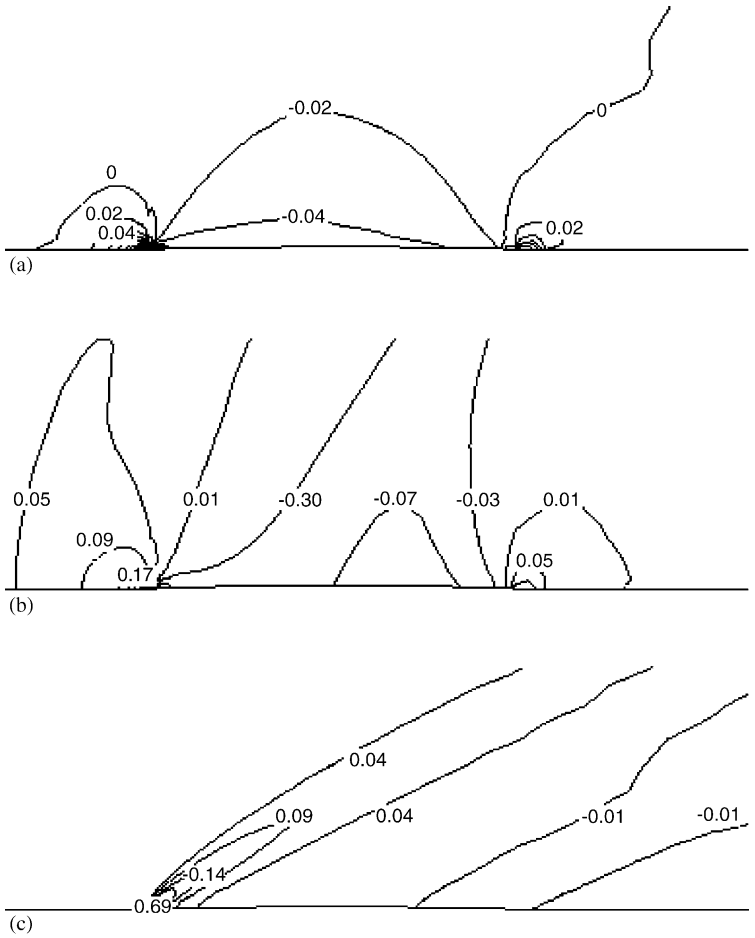

Fig. 4. Pressure contours for panel for Mach: (a) 0.3, (b) 0.8 and (c) 2.0.

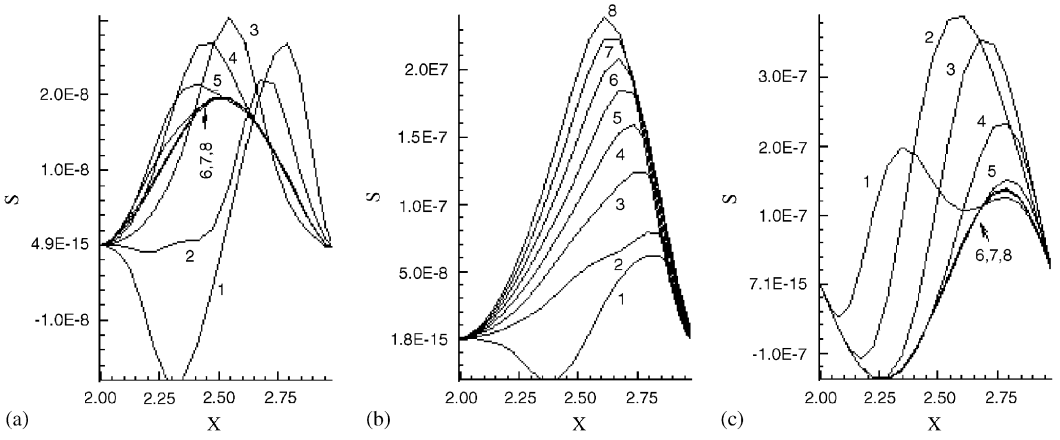

Fig. 5. Displacements s(m) for panel after $1, 2, ..., 8$ time units for Mach: (a) 0.3, (b) 0.8 and (c) 2.0.

6. Conclusions

A method based on ALE in finite difference for modeling panel fluid–structure interactions was developed. It can be employed for high-order space and time approximations for solving even more complex fluid–structure interaction situations. Therefore, the general approach can be extended to big displacements.

The code has been calibrated when computing subsonic and transonic flows around airfoils (De Bortoli, 2002); the structural deflections were compared with analytical values. Since explicit time-stepping schemes are used, the solution algorithm is obviously easily vectorizable and parallelizable.

Results indicate that the amplitudes of deflections grow when increasing the flow velocity. Besides, a rigid panel, with big elasticity modulus, can be employed to verify implementation errors, when they exist; such a case showed very small amplitudes.

The results indicate the tendency of a clamped panel to lose stability by divergence in the subsonic regime and by flutter in the supersonic case. The code is being extended to solve aeroelastic problems over more complex flexible geometries using simpler methods.

Acknowledgements

The author would like to thank to Prof. Mark Thompson for reading the paper and for some comments. Part of this work was developed under the sponsorship of CNPq (Process 310010/2003-9).

References

Belytschko, J., Hughes, T.J.R., 1986. Computational Methods for Transient Analysis. North-Holland, New York.

Bisplinghoff, R.L., Ashley, H., Halfman, R.L., 1957. Aeroelasticity. Addison-Wesley Publishing Company.

Blazek, J., 1994. Verfahren zur Beschleunigung der Lösung der Euler und Navier–Stokes Gleichungen bei Stationaren Über- und Hyperschallströmungen. Ph. D. Thesis, University of Braunschweig, Germany.

De Bortoli, A.L., 1994. Solution of incompressible flows using compressible flow solvers. DLR IB 129/94-18, Braunschweig, Germany, pp. 1–86.

De Bortoli, A.L., 2002. Multigrid based aerodynamical simulations for the NACA 0012 airfoil. Applied Numerical Mathematics 40, 337–349.

Försching, H.W., 1974. Grundlagen der Aeroelastik. Springer, Berlin.

Garrad, A.D., Carpenter, P.W., 1982. On the aeroelastic forces involved in aeroelastic instability of two-dimensional panels in uniform incompressible flow. Journal of Sound and Vibration 80, 437–439.

Guruswamy, G.P., 1990. Unsteady aerodynamic and aeroelastic calculations for wings using Euler equations. AIAA Journal 28, 461–469.

Jameson, A., Schmidt, W., Turkel, E., 1981. Numerical solution of the Euler equations by finite volume methods using Runge–Kutta time-stepping schemes. AIAA Paper, 81–1259.

Kroll, N., Rossow, C.-C., 1989. Foundations of numerical methods for the solution of Euler equations. Prepared for Lecture F 6.03 of CCG, Braunschweig, Germany.

Marshall, J.G., 1996. A review of aeroelasticity methods with emphasis on turbomachinery applications. Journal of Fluids and Structures 10, 237–267.

Souli, M., Ouahsine, A., Lewin, L., 2000. ALE formulation for fluid–structure interaction problems. Computer Methods in Applied Mechanics and Engineering 190, 659–675.

Usab, W.J., Murman, E.M., 1983. Embedded mesh solution of the Euler equation using a multiple grid method. AIAA Paper 83-1946-CP.